A Hardware Space Elevator Simulator

Dennis H. Wright[1]
SLAC National Accelerator Laboratory, Stanford, CA, 94025

Several calculations of space elevator motion have been made, and development of a software simulator will begin in the near future. To date however, there are no mechanical simulators which can reproduce space elevator motions in the laboratory so that theoretical predictions can be validated. By analogy to wind tunnels, such mechanical simulation is necessary if critical space elevator motions are to be tested on Earth before testing in space.

This paper examines the possibility of building a gravity analog simulator in which transverse and longitudinal vibrations of the space elevator can be tested on a scaled-down version of the Earth-tether-climber system. The goal is to design a simulator in which as many space elevator parameters as possible can be varied and tested on a laboratory scale and compared to software predictions. It will be shown that gravitational stabilization, oscillations in the orbital plane due to climber motion and other perturbations, extensions of the tether due to various stresses, and certain tether failure modes such as parting due to debris impact, can be demonstrated faithfully.

The paper concludes that a research-quality simulator could be built on the scale of about 10 meters using conventional centrifuge and air cushion technology.

Nomenclature

CCD	=	charge coupled device
E	=	Young's modulus of a material
ε	=	extension strain
dr	=	increment in radius
F_C	=	centrifugal force
F_g	=	analog of gravitational force in simulator
GEO	=	geosynchronous orbit
H	=	dimensionless constant used to scale the gravitational potential
g	=	acceleration due to gravity at the surface of the Earth = 9.81 m/s^2
r	=	radius of funnel shape and distance from center of Earth
rpm	=	revolutions per minute
R_E	=	Earth radius
R_G	=	radius of geosynchronous orbit
ρ	=	bulk material density in kg/m^3
σ	=	mechanical stress in MPa
ω	=	angular velocity in radians/s

I. Introduction

BEFORE any part of the space elevator is deployed, it will have to be simulated both in software and in hardware. Many calculations and software simulations have been done, or are planned to be done[1] so that a good understanding of space elevator dynamics will be accumulated. Each of these calculations will need to be validated by experiment or hardware simulation in much the same way that wind tunnels are used validate certain aerodynamic calculations.

[1] Physicist, Particle and Particle Astrophysics Department, SLAC, dwright@slac.stanford.edu

Hardware simulations of the space elevator present unique challenges. First among these is the necessity to model the space elevator on a scale that permits Earth-based testing. Length, mass, tether parameters, rotation rate and the gravitational field in which the space elevator operates all need to be appropriately scaled down so that the motions to be studied are faithfully reproduced in the laboratory.

It is unlikely that a single method will be found which can simulate all of the motions and parameters that need to be studied, so a collection of methods should be considered. For example, a tether suspended down a deep vertical mine shaft[2] would provide good tests of longitudinal and transverse oscillations, both in and out of the orbital plane, as well as the effect of tether climbers, but the force of gravity would not vary enough over the tether length to study gravitational effects, nor could Coriolis effects be tested. A rotating, thin, flexible charged wire in a laboratory-generated electromagnetic field could be used to simulate the effects of gravity, Coriolis effects and the magnetosphere on the tether, but the field itself would be rather complex and the volume in which it must be provided would entail large and expensive magnets.

The method proposed here will employ a combination of centrifuge and air table technologies to simulate the Earth's gravity well and rotation, the extension and in-orbital-plane transverse vibrations of the tether, and climber motions. It is likely that such a simulator would be small enough to fit into an experiment hall, yet large enough to reproduce most of the important space elevator motions.

II. Gravity Analog Devices

Devices which simulate motion in a gravity well on a small scale are already in operation in science museums. A particular type[3] is shown in Fig. 1. The demonstration begins when a coin is launched onto the outer edge of a funnel-shaped surface of revolution. The coin rolls along the surface, tracing an orbit around the central hole of the device. The radius of the coin's orbit gradually decreases, due to friction and air resistance, and the coin eventually falls into the central hole. Without friction or air resistence, the coin would continually orbit the central hole, just as a satellite orbits the Earth.

The key to this type of demonstration is that the force which draws the coin towards the center, when projected onto a plane parallel to the floor, can have the same functional form as classical gravitation. For this reason such devices are often referred to as gravity analogs. If we now replace the coin with a string of beads, with each bead able to rotate about the string axis, and set the string in motion along the surface of the simulator so that one end of the string is near the central hole and the other end is near the outer radius, we begin to approximate the space elevator tether. Depending on the rotational velocity of the string and the depth of the analog gravity well, the string of beads will achieve a stable configuration in which it is stretched taut along the surface of the well, and when seen from above, will appear to be a straight line extending from the central hole to the outer radius. The motions of the individual beads relative to the string axis simulate the vibrations of the space elevator tether. These motions could then be photographed and stored for later comparison to theoretical predictions.

In order to develop this concept into a practical simulator, a number of practical issues must be dealt with, including the determination of the properly scaled rotational velocity and gravity well depth, the reduction or elimination of friction and air resistence, and the mechanical modeling of the tether and climber.

Figure 1. Gravity well simulator produced by HyperbolicFunnel Company.

III. Well Depth and Rotational Velocity

The shape and depth of the funnel can be determined by calculating the balance of forces on a point mass constrained to move in a stable orbit along the funnel's surface. For the time being, friction and air resistence will be neglected. Figure 2 shows the shape of the funnel and the relevant forces on the point mass.

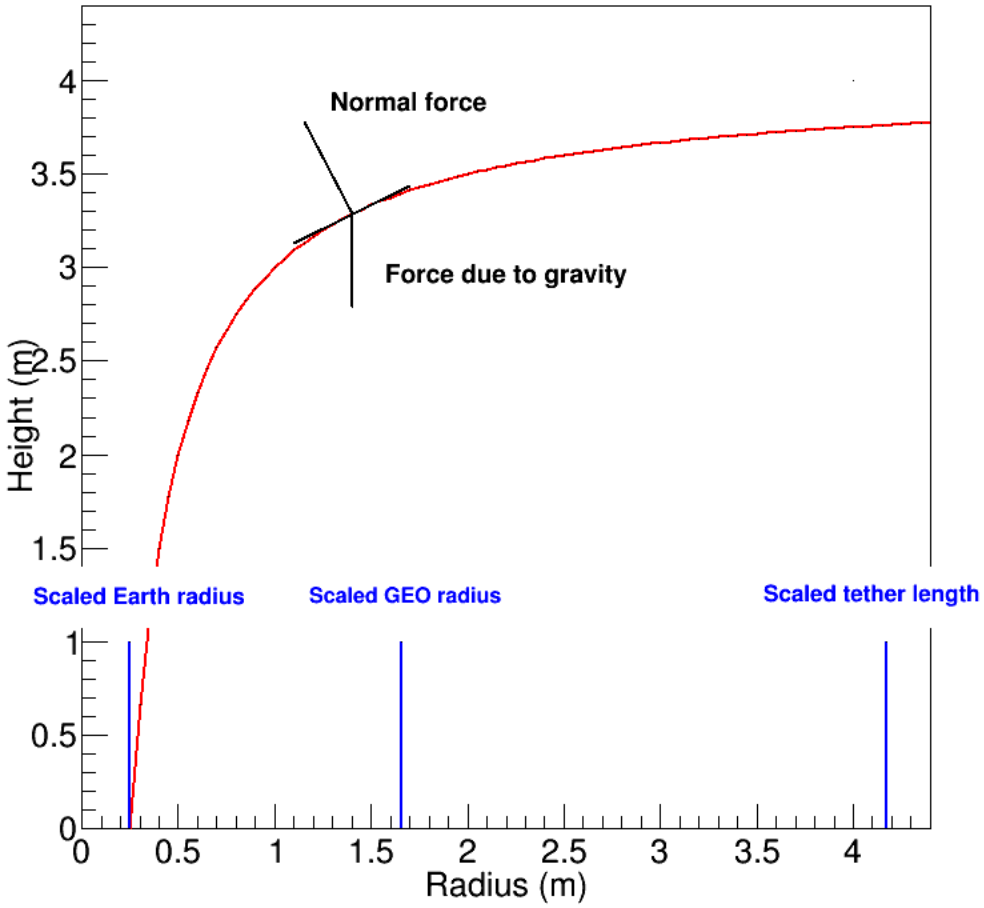

Figure 2. A cross section of the funnel's surface is shown by the red curve. Black lines show the slope of the surface, the normal force exerted perpendicular to the slope, and the downward force of gravity. Blue lines indicate the scaled Earth and geosynchronous radii, and the apex of the tether.

Similar to the forces on a ball rolling down an inclined plane, the normal force exerted by the surface on the mass is $mg/\cos\theta$. The upward component of the normal force is then just mg, exactly balancing the downward force of gravity. The horizontal component of the normal force is

$$mg\ \sin\theta/\cos\theta = mg\tan\theta = -mg\frac{dU}{dr}\ , \tag{1}$$

where dU/dr is the derivative of the function representing the funnel shape. For our simulator, $U(r)$ is the red curve of Fig. 2 and is given by

$$U(r) = H\left[R_E - \frac{R_E^2}{r}\right], \tag{2}$$

where r is the distance from the vertical axis of the funnel, R_E is the radius of the Earth as scaled down to fit the simulator and H is a dimensionless constant which we later use to scale the simulated gravity. Thus for any point on the surface of the funnel, the horizontal component of the force is given by the derivative of the potential

$$F_g(r) = -mg\frac{dU}{dr} = -mgH\frac{R_E^2}{r^2} \ . \tag{3}$$

Here the minus sign indicates that the force is always directed inward toward the axis of the funnel. Except for a scale factor, this exactly reproduces the gravitational force seen by a body at a given distance from the Earth. If the body orbits at an angular velocity ω at a distance r from the funnel axis, the centrifugal force will be

$$F_C = m\omega^2 r \ , \tag{4}$$

directed parallel to the laboratory floor and away from the funnel axis. To keep the point mass at a constant radius requires that the net horizontal force acting on it be 0, or $F_g + F_C = 0$, from which follows

$$\omega^2 r = gH\frac{R_E^2}{r^2} \ . \tag{5}$$

At the geosynchronous radius R_G in the simulator, the angular velocity is then given by

$$\omega = \sqrt{gHR_E^2/R_G^3} \ . \tag{6}$$

Since the Earth radius will be scaled down to laboratory size, the geosynchronous radius must be scaled down by the same factor if the orbital dynamics are to be faithfully reproduced. Therefore $R_G = 6.618\ R_E$, and

$$\omega_{GEO} = \sqrt{\frac{gH}{290\ R_E}} , \tag{7}$$

so that the angular velocity of the point mass at simulated GEO now depends only on the simulated Earth radius, the gravitational acceleration in the laboratory and the scaling variable H. Once the simulated tether is in place and stable, it will also rotate at this rate.

Experimental considerations can now be used to determine R_E , H, and therefore ω. R_E and H determine the radius and depth of the simulator funnel through Eq. (2). The radius is our chief concern because it determines the length of tether than can be simulated and the size of tether oscillations that can be studied. Obviously the bigger, the better, but limits are imposed by practical considerations. The ultimate limitation comes from the ability to image and record transverse oscillations and deflections of the simulated tether. The smallest deflections that will likely be of interest are those caused by the Coriolis force due to the climber ascending and descending the tether. These are of order 0.2 km according to Ref. 4. The smallest deflections that can be imaged in the laboratory will be limited by optics and the quality of the cameras. Assuming high quality CCD cameras, a rough estimate of the smallest image size is given by

$$S = M\frac{\lambda}{2n\sin\theta} \ , \tag{8}$$

where S is the image size in μm, M is the magnification and λ is the wavelength of light in μm. $n\sin\theta$ is the numerical aperature of the device and is typically about 1.4. For a magnification of 40 and λ = 0.55 μm for green light, S is about 7.86 μm. The scaled-down length of the tether can now be found, assuming a full scale tether length of 100,000 km :

$$L_{lab} = \frac{7.86\ \mu m}{0.2\ km}100{,}000\ km = 3.93\ m \ . \tag{9}$$

On the same scale the radius of the Earth would be 0.25 m and the geosynchronous orbit radius would be 1.65 m. These radii and the tether apex distance are shown in Fig. 2.

Now it remains to set the depth of the funnel. For the red curve in Fig. 2 the factor *H* of Eq. (2) was set to 16 so that the depth of the funnel is about the same as its radius. This is an arbitrary choice which can be modified as necessary to produce the optimal rotation rate of the tether and the force pressing it to the funnel surface. The rotation rate is then

$$\omega = \sqrt{\frac{16\ (9.81\ m/s^2)}{290\ (0.25\ m)}} = 1.47\ s^{-1} = 14\ rpm\ . \qquad (10)$$

At this rate, a tether stretched along the surface of the funnel would feel a horizontal acceleration of 16 g at $r = R_E =$ 0.25 m and 0.057 g at the apex of the tether. The downward acceleration of course remains 1 g at all radii.

IV. Friction and Air Resistence

Whether the simulated tether slides along the surface of the funnel, or rolls if it consists of a string of beads, friction will likely be large enough to destroy any precise reproduction of tether dynamics. A possible solution to this problem would be to use an air cushion such as that used in the textile industry[5] (Fig. 3), arcade games or high school physics demonstrations. The tether would then move freely along the surface and its oscillations would not be impeded. For a gravity simulator, the pneumatic surface would be funnel-shaped, following the function of Eq. (2). This requires an adaptation of the standard air table design.

Figure 3. Pneumatic cushion table used in the textile industry.

For a flat table, the holes through which air is forced are uniformly distributed over the surface and the air pressure from the pump is constant everywhere. For a funnel-shaped surface, however, the distance between the holes will need to decrease as the funnel radius decreases, assuming a constant pump pressure at each hole. This distance as a function of radius can be calculated so that the force of air perpendicular to the surface exactly counteracts the centrifugal and gravitational forces at any point along the tether. The average areal density of the holes is a parameter which will have to be determined experimentally. It will have to be large enough that there are no significant non-uniformities in the air cushion, and small enough to make construction practical.

There remains the problem of air resistance. The simulated tether, though small in width and thickness, will still encounter enough air resistance to slow it down and distort its orbital dynamics, especially if the tether rotation rate is high. Up to now, we have considered a system in which the tether was rotating about the central axis of a non-rotating funnel. If the funnel were to rotate at the same rate as the tether, and a sector of the funnel were to be closed off so that the air inside it would rotate as well, the tether would experience very little air resistance. In fact, it would be unnecessary to construct the entire funnel, but just a sector instead. This would greatly reduce the materials and cost of the simulator. A funnel sector spanning 45^{o} would be sufficient to study very large tether oscillations, including failure modes.

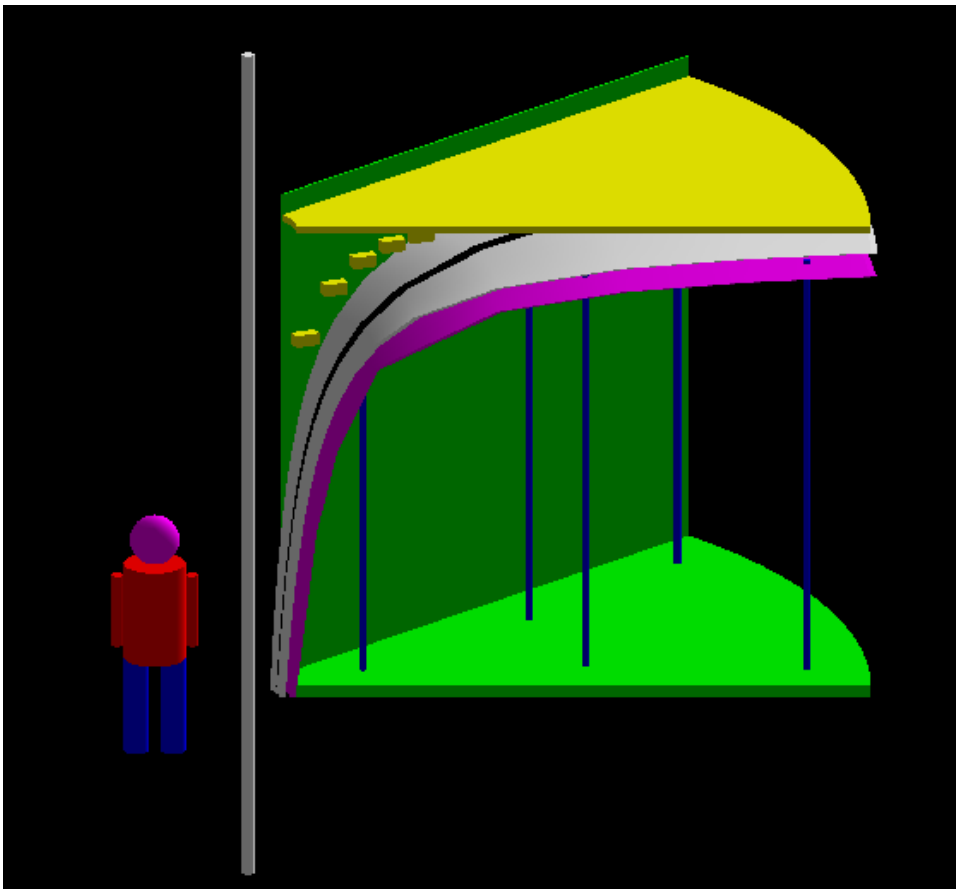

Figure 4. Space elevator simulator. The curved white surface is a 45^{o} sector of the three-dimensional surface of revolution of Eq. (2) with H = 16 and R_E = 0.25 m. It is perforated with small holes which provide the pneumatic cushion on which the tether (black) floats. The magenta surface beneath it supports and contains the forced air ducting. The yellow sector at the top is an instrumentation platform from which are suspended cameras (yellow boxes) which photograph the tether. This platform also supports servo-mechanisms to place the tether. All but one of the vertical air containment panels (green) have been removed to show the interior. The entire mechanism rotates about the vertical axis shown by the white pole.

Figure 4 shows what such a device might look like. The base of the simulator would resemble the arm of a centrifuge, which would either be supported as a cantilever or rest on circular rails as it travels around its central pivot. On the base would be built a 45° sector of the funnel with the cross sectional shape of Eq. (2). Vertical walls placed at each edge of the sector would reduce air motion near the tether. Resting on the walls would be an instrumentation platform to support the CCD cameras which photograph the tether and the servo-mechanisms which lower and release the tether onto the funnel surface.

V. Modeling the Tether

The orbital dynamics of the tether do not depend on its absolute mass (unless it is very large), but rather on its relative mass distribution. Hence the total tether mass need not scale, nor does the density of the material used to make it. This allows us to choose the total mass of the modeled tether so that it does not float away from the air cushion, nor make contact with the funnel surface. Once the mass is determined, the dimensions of the modeled tether can be chosen accordingly.

Building an exactly scaled, laboratory-sized version of the full tether would be impossible. Using the scaling factor of about 39 parts per billion established in Eq. (9), a maximum tether width of six meters reduces to 0.23 μm. The typical full scale tether thickness, which will likely be less than 1 mm, would be reduced to about 0.04 nm. Fortunately, an exact scaling of all the dimensions is unnecessary. Since only the relative mass distrubtion is important, at least two options are open to us. The first option models the tether as having a constant density material, a constant thickness, and a width which varies according to the Pearson taper[6],

$$W(r) = W_0 \, exp\left[\frac{R_E^2}{hR_G}\left\{\frac{3}{2} - \frac{R_G}{r+R_E} - \frac{1}{2}\left(\frac{r+R_E}{R_G}\right)^2\right\}\right] . \tag{11}$$

The width dimension extends parallel to the funnel surface, while the thickness dimension is perpendicular to it. One problem with this option is that the width varies in the simulated orbital plane, thus disproportionately affecting the oscillation amplitude. If the modeled tether material happens to be relatively stiff, oscillations will be additionally distorted. The varying width also poses a problem if masses need to be attached to and slide along the tether as when climbers are being modeled.

The other option assumes the tether has a cross section constant along its length, but with its bulk density instead of its width varying with length as in Eq. (11). This option allows things to slide easily along the tether, but is likely more difficult to construct. Varying density may also contribute to varying stiffness and thus distort the oscillations.

The material of the modeled tether should be both flexible and extensible. The full tether, although locally very stiff due its high Young's modulus, will appear very flexible over its entire length. Given its specific strength it will also be extensible, such that in its steady state, its length will stretch by about 3.5%. For the simulated tether we aim to match this flexibility and stretching so as to reproduce longitudinal oscillations as well as transverse ones.

The expected amount of stretching of a material is given by

$$\varepsilon = \frac{\sigma}{E}, \tag{12}$$

where σ is the stress and E is the Young's modulus. The stress is the tension at a point along the tether, divided by the cross sectional area at that point. The stress at radius r can be found by rewriting Eq. (5), multiplying by the bulk density ρ and integrating from R_E to r, to get

$$\sigma(r) = \rho H g R_E \left[\left(1 - \frac{R_E}{r}\right) + \frac{1}{580}\left(1 - \frac{r^2}{R_E^2}\right)\right]. \tag{13}$$

For many carbon compounds, including carbon nanotubes, ρ is about 1300 kg/m^3 . Taking H = 16 and R_E = 0.25 m as above, g = 9.81 m/s^2 and $r = R_G$ = 1.65 m gives a stress of 39,540 kg/m/s^2. To get an extension of 3.5% a Young's modulus of 1.13x10^6 kg/m/s^2 = 1.13 MPa would thus be required. Silicone rubber has a Young's modulus between 1 MPa and 50 MPa, and a density between 1100 and 2300 kg/m^3 so it would be a candidate for the simulated tether material.

A discretized model of the tether, such as a string of small beads, could also be considered. The mass of each bead could be chosen to have the scaled mass of the corresponding segment of the full tether. This would be easy to manufacture, but a large number of beads would be required to reproduce relatively small oscialltions, stretching could not be modeled, and it would be more difficult to implement simulated climber motion.

VI. Launching the Simulation

While the simulator is rotating at the desired rate, servo-mechanisms mounted on the instrumentation platform grip the tether, shape it to conform to the funnel surface, and stretch it to match the extension it would experience at this rotation rate. Viewed from above the tether would extend radially in a straight line from the innermost funnel radius to its full length near the outer edge. The servos then lower the tether to the funnel surface and gently release it. At this point, each particle of the tether should now be traveling at the same local velocity as the funnel beneath it and the air surrounding it. Centrifugal force and gravity keep the tether stretched and near the funnel surface, and the air cushion keeps it from contacting the surface so that its momentum is preserved. The tether should now orbit indefinitely in the funnel as long as the rotation rate and cushion air pressure are maintained.

Once the simulation is underway, several actions could be taken in order to study the response of the tether. To simulate the effect of impulses along the tether, the servos can be used to give the tether a kick at any point along its length. This could be done after the tether has stabilized in its orbit, or as the tether is initially released onto the funnel surface. The effect of a climber could be simulated by a small steel bead which slides along the tether and is drawn by a magnet traveling at the proper velocity along the instrumentation platform. It is estimated that a climber will take about one week[7] to reach GEO. Scaled to the simulator discussed above, the climber bead would be moved along the tether at a velocity of about 1.4 m/ 30 s = 4.7 cm/s.

Tether severance scenarios could be studied by having the servos cut the tether, but carefully so that unphysical motions of the cut ends are not introduced. Deployment simulations are also conceivable, but it may be difficult to construct a device which could pay out both a descending and ascending tether, be remotely controlled, and small enough that it would not interfere with simulated motion.

Once each of the above simulations has begun, cameras will record tether motion at every point along its length. The number of photographs taken during a simulation would depend on the tension in the simulated tether, but a rate of a few frames per second should be sufficient for the conditions postulated above. Once taken, each photo will be digitized and stored electronically for later analysis.

VII. Limitations

Although many aspects of tether motion can be studied with this simulator, a number of features cannot, due to choices made in its design and limitations brought about by the large scaling factor. Because the simulated tether should always conform to the funnel surface, only oscillations in the orbital plane can be studied. In addition, the smallest frequency transverse oscillations that can be observed are limited by the large scaling factor of the tether length. The Young's modulus of the simulated tether material is very small compared to that of the full tether. This, combined with the small tether length means that no simulation of bending is possible. The same is true for torsion. Perturbations of tether motion due to lunar and solar gravity and electromagnetic fields from the magnetosphere will be very difficult to simulate unless large magnets can be made which contain the entire simulator and act on a current-carrying tether.

VIII. Conclusion

A laboratory-sized mechanical simulator of space elevator motion can be built by forming an air cushion into the shape of a funnel and placing this on the arm of a centrifuge rotating at about 14 rpm. A funnel five meters in radius and four meters in height will be sufficient to test a model of the space elevator at a scale of 1:25,600,000. The tether will be constructed of a string of silicone rubber, with a linear mass density varying along its length according to the Pearson taper formula. A magnetically drawn bead sliding along the tether will represent the climber. While the model tether and climber float on the air cushion, oscillations may be introduced by servo-mechanisms mounted on a platform above the funnel surface. These motions will be photographed by cameras mounted on the same platform. For a device of this size it is estimated that deflections of the tether as small as 5 – 10 μm can be measured, allowing most of the important space elevator motions to be studied and compared to theoretical predictions.

References

[1]Wright, D.H., Avery, S., Knapman, J., Lades, M., Roubekas, P., Swan, P.A., "Design Considerations for a Software Space Elevator Simulator," ISEC Position Paper #2017-1, Lulu.com, 2017.

[2]Robinson, P., discussion at ISEC Conference, 2014.

[3]Kantz, W.E., The hyperbolic funnel, www.hyperbolicfunnel.com .

[4]Ohkawa, R., Uchiyama, K. and Fujii, H.A., "The Effect of Disturbance on Space Elevator Dynamics with Flexibility," 61st International Astronautical Congress, Prague, IAC-10-D4, 4.5, 27 Sept. – 1 Oct. 2010.

[5]Rexel Company, Air cushion table, www.rexelpoland.com .

[6]Pearson, J., *Acta Astronautica* 2, 785-799 (1975).

[7]*Space Elevators: An Assessment of the Technological Feasibilty and the Way Forward*, Eds. Swan, P.A., Raitt, D.I., Swan, C.W., Penny, R.E. and Knapman, J.M., p. 63, International Academy of Astronautics, 2013.